Communications in Mathematics and Applications
Vol. 15, No. 1, pp. 203–219, 2024
ISSN 0975-8607 (online); 0976-5905 (print)
Published by RGN Publications
DOI: 10.26713/cma.v15i1.2373

http://www.rgnpublications.com

Research Article

Computational Simulation and Modelling of Arterial Drug Delivery From Half-Embedded Drug-Eluting Stents in Single-Layered Homogeneous Vessel Wall

Ramprosad Saha[1], Somnath Choudhury*[2] and Akash Pradip Mandal[3]

[1] *Department of Mathematics, Suri Vidyasagar College* (*affiliated to the University of Burdwan*), *Suri 731101, West Bengal, India*
[2] *Department of Physics, Suri Vidyasagar College* (*affiliated to the University of Burdwan*), *Suri 731101, West Bengal, India*
[3] *Department of Mathematics, Ananda Chandra College* (*affiliated to the University of North Bengal*), *Jalpaiguri 735101, West Bengal, India*
***Corresponding author:** somnathbratati21@gmail.com

Received: August 15, 2023 **Accepted:** December 12, 2023

Abstract. The next-generation of drug therapics has started as a consequence of the invention of controlled-dose pharmaceutical delivery tools. More specifically, coronary angioplasty (CA) treatments often involve drug-eluting stents (DESs) that eluting drug molecules. This mechanism decreases the in-stent restenosis with the help of releasing drugs from a thin polymer membrane covering into the coronary vessel tissue around it. Present day DES equipments, as the protective covering, biodurable polymers has been deployed, that, remains there forever until the drug has fully eluted from DES. In this present work, we investigated the aforementioned problems using a numerical simulation of vascular distribution of drugs as well as receptor binding mechanisms. Modelling is done for the intravascular drug delivery of a hydrophobic (like sirolimus or paclitaxel) drug from DES. The content of this paper discusses the effects of drug delivery from half-embedded circular drug-eluting stent struts. We introduce an elaborate mathematical approach based on axi-symmetry 2D layout, incorporates a two non-linear phases of drug binding namely specific and non-specific, and combines the impact of diffusion and advection, within the single-layered homogeneous vessel wall. The pharmaceutical delivery via five stent struts has been significantly strengthened in this framework. The free pharmaceuticals are moved using an unsteady covection-diffusion-reaction mechanism, even though the binding pharmaceuticals are being through an unsteady reaction-diffusion mechanism. The governing equations along with the initial and boundary conditions has been evaluated numerically using a finite-difference technique in staggered grids. The marker and cell (MAC) methodology has been employed to solved the model equations while taking into account the cylindrical system of polar coordinates. In this present assessment, our target is to visually illustrate the impact of the embedment of the stent on the drug release from stent and vessel drug distribution. According to the findings, it is indicate that the drug gradually binds to specific receptors and extracellular matrix sites until binding sites become saturated. Model simulations have improved our understanding of the potential influences of the different factors that may affect the effectiveness of drug administration. The created modelling allows for the modification of the model's parameters for upcoming research on the development of PLGA-coated drug-eluting stents.

Keywords. Cardiovascular tissue wall, Half-embedded DES, Specific binding, Non-specific binding, Marker and cell (MAC) method

Mathematics Subject Classification (2020). 35Q92, 65M06, 76A05, 76D05, 80A19, 92B05

1. Introduction

Coronary artery disease (CAD) is the number one cause of death worldwide (Roth and others [10]). *Percutaneous coronary intervention* (PCI), in which a DES is implanted in order to broaden narrowed vessel and enhance the circulatory function, is becoming increasingly effective therapy for severe CAD. At present, the overwhelming percentage of DES used to provide pharmaceutical to the wall of vessel to reduce inflammation after deployment in an effort to avoid uncontrolled neointimal regeneration, or restenosis. Following coronary angioplasty treatments, drug-eluting stents have demonstrated significant advantages in preventing *in-stent restenosis* (ISR). This system helps a long-term pharmaceutical delivery like sirolimus or paclitaxel, that are embedded within the vessel wall and released from polymeric coating and may inhibit a specific phases of progression of ISR (Costa and Simon [8]). However, the numerous aspects make stent design more challenging and assessment and hampered the advancement of DES.

The purpose of drug-eluting stents is better understood through the use of modelling and simulation technique, which can also help to increase the effectiveness of medical equipment. The release from drug coated stent and drug-vessel tissue interactions were investigated in one-dimensional simulations by Hossainy and Prabhu [13]. Drug transport by convection and diffusion process through the vessel wall for both the hydrophilic and hydrophobic drug mass have been evaluated (Hwang *et al*. [15]). A relevant fluid dynamics computation and drug transport system has been used to examine the influence of thrombus (Balakrishnan *et al*. [2]), blood flow (Borghi *et al*. [6]), stent coating (Balakrishnan *et al*. [3]), and strut position (Balakrishnan *et al*. [4]) on stent-based drug delivery for a single strut in the longitudinal pattern of the artery. A bi-layered polymer covered stent was shown to be the most successful in the cross sectional study of drug elution from an entire embedded stent strut (Grassi *et al*. [11]). In order to investigate the effects of various strut shapes drug diffusivities on vascular pharmaceutical absorption, system with multiple struts were also established (Mongrain *et al*. [22]).

To analysis the drug-release mechanism and binding dynamics, as well as to improve the stent geometry and physio-chemical factors, mathematical and computational (in vivo) simulation has become a very important role (Bozsak *et al*. [7], and McGinty [16]). But in vivo system by themselves are insufficient. For this issue is to be completely addressed, a variety of simulations, covering everything from in vitro to ex vivo, are necessary (McKittrick *et al*. [20]). Several in vivo system value assumptions can be established through practical in vitro and ex vivo research, but in vivo measurements of drug leaving on the stent and in the tissue are often required for confirming the simulation (Tzafriri *et al*. [25]).

There is an enormous amount of investigations, especially, on the mathematical and computational simulation of DESs (McGinty *et al*. [17]). Research of Tzafriri *et al*. [25, 26] has emphasised the significance of involving of two phases of nonlinear drug binding (specific and non-specific) within the frameworks, with saturation of specific receptors having been extremely associated with effectiveness, particularly sirolimus-eluting stents. The fact is that these representations were made easier as they only took into account one dimensional model, unlike the complicated physics and biology that underline them. Many layers of vessel wall are currently included in the most sophisticated two-dimensional axi-symmetry formulations

of DES kinetics, which are more a perfect version but nonetheless more accurate than earlier versions (Escuer *et al*. [9]). However, their main objective was to offer an analytical solution, which called for the simplification of other factors such as the binding model's dimensionality and linearity.

The most comprehensive conceptual framework for drug delivery from half-embedded drug-eluting multiple stent struts, drug transpot and retention to date is presented in the present article. We consider a single-layered homogeneous vessel wall with a two-dimensional axi-symmetry shape, two nonlinear phases of drug binding (specific and non-specific), and influence of advection. In this manuscript, we employed the MAC method in spacial discretization and the forward time central spaced discretization technique for solving the governing equations. Here, we expand the study done on the customised use of cardiovascular half-embedded drug-eluting stents to assess the value of constructing both the specific and non-specific binding structures where saturation is achievable within the single-layered homogeneous vessel wall.

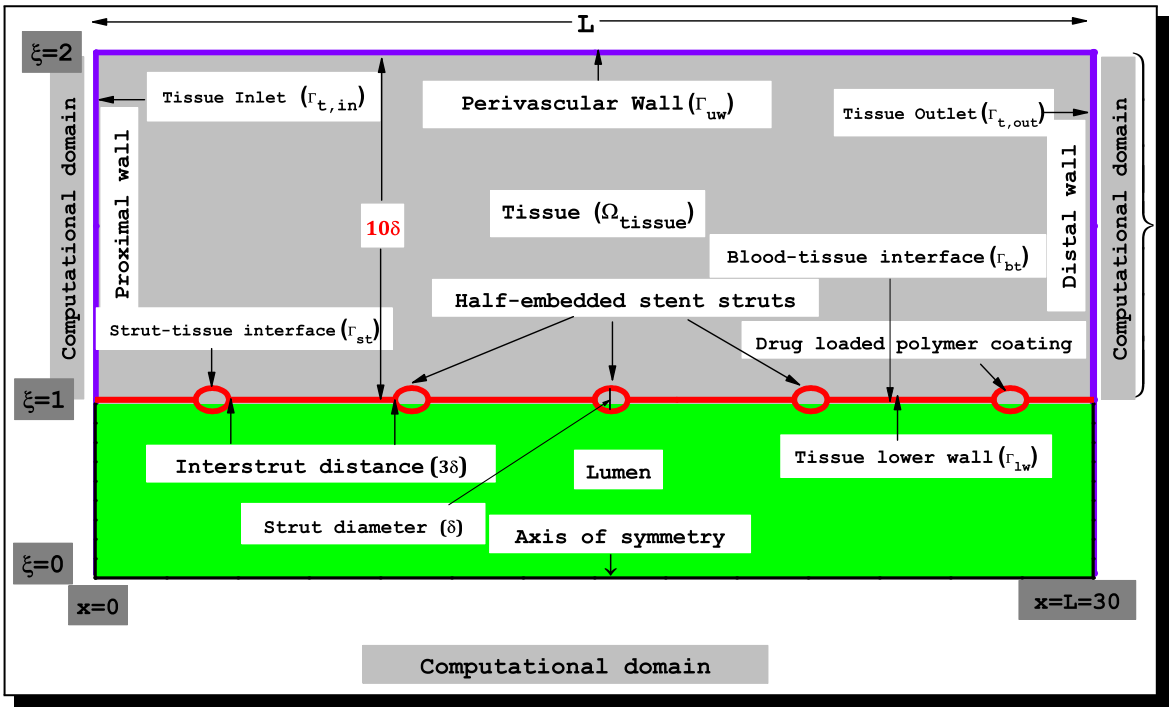

Figure 1. Computational model geometry which we have used

2. An Overview of Stent Design Demonstrating

We studied the vascular drug concentration acquired by *sirolimus eluting* (SES) because they offer both mono-phasic and bi-phasic elution characteristics. In this investigation, a straightforward Cardio Coil stent with a circular strut was utilised (Acharya and Park [1]). Considering the fact that multiple struts each of 0.1 mm in diameter, are placed with inter-strut distance of 0.3 mm. In the present setup, five half-embedded drug-eluting stent struts were been employed. Here, we considered the artery's diameter is 3 m while the vessel wall's thickness and the thickness of the polymer coating of DES are 0.9 mm and 0.005 mm respectively. The two-dimensional form shown in Figure 1 is taken into account as the DES is axi-symmetry.

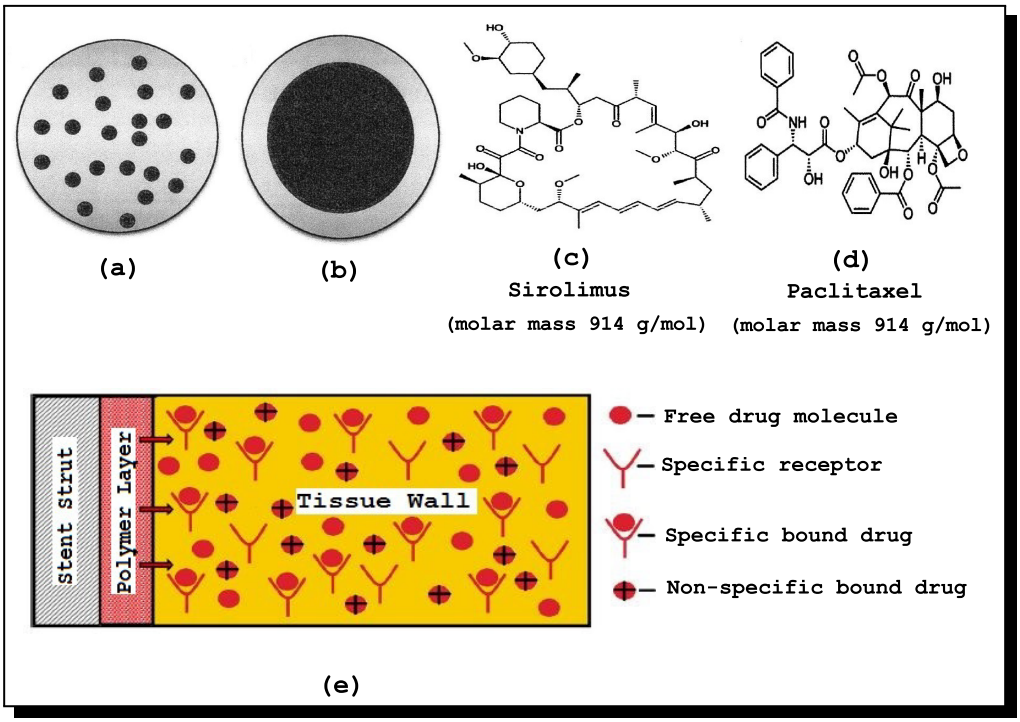

Figure 2. In a matrix configuration: (a) drug is uniformly dispersed; in a reservoir configuration; (b) a drug core is contained in a polymeric shell; (c) molecular structures of sirolimus and (d) paclitaxel. Both drugs are very hydrophobic, (e) geometrical representation of polymer coated *drug eluting stent* (DES), polymeric layer, arterial tissue wall, unbound drug in free phase, bounded drug binds to non-specific general *extracellular matrix* (ECM) sites (ECM-bound) and binds to specific receptors (SR-bound) ([19,29])

3. Introduction to the Problem Formulation

The following section proposes a 2D-representation of the drug delivery strategy (McGinty and Pontrelli [18]) of cardiovascular stent struts circular in shapes, which illustrates how the drug diffuses within the vessel wall. Upgrade the framework in this latest schematic to include two distinct binding phases inside the vessel wall.

3.1 Concentration-Releasing Process Through the Polymer Covering

Depending on the mechanics of drug release, the polymeric controlled-release systems for delivering drugs may be grouping generally into different types such as diffusion controlled systems, chemically controlled systems, solvent activation controlled systems etc. The two preferred choice for polymer delivery methods are the matrix-based method and reservoir-based method (Figure 2(a,b)). The biochemical properties of relevent drugs adopted in DES treatments like sirolimus and paclitaxel are addressed here (Figure 2(c,d)). We analyse an improved 2D scenario (Figure 2(e)) in this arrangement since the majority of the mass delivery happens in the path corresponding to the tissue wall. We have considered the matrix-embedded pool of drug release is anticipated to follow the Higuchi tupe diffusion-based dissolved process (Higuchi [12]). Therefore, the specifications for continuous sirolimus elution kinetics through DES stent coating were expressed as follows:

$$C_s(0) - C_s(t) = M_0(1 - e^{-K_0 t}) + H_s\sqrt{t} \quad \text{on} \quad \Omega_{tissue} \cap \Gamma_{st}\,, \tag{3.1}$$

in which $C_s(0) = C_0$ represents the initial load of drug per stent; M_0 is the initial pool of first order eluting drug, with rate constant K_0, and H_s is the Higuchi rate constant (McGinty and Pontrelli [18]).

3.2 Modelling of Drug Delivery Procedures

The transportation of the free drug concentrations withion free phase inside the vessel wall may be written as advection-diffusion equation (McGinty and Pontrelli [19]):

$$\frac{\partial C_{fd}}{\partial t} + \frac{\partial (V_w C_{fd})}{\partial y} + \frac{\partial C_{bed}}{\partial t} + \frac{\partial C_{brd}}{\partial t} = D_w \left[\frac{\partial^2 C_{fd}}{\partial x^2} + \frac{1}{y}\frac{\partial C_{fd}}{\partial y} + \frac{\partial^2 C_{fd}}{\partial y^2} \right], \tag{3.2}$$

in which t denotes time since stent implantation, x and y are the axial and radial coordinates with dimension, respectively, $C_{fd}(x, y, t)$, is the is the molar concentration of free drug per unit tissue volume within side the arterial wall; D_w denotes the transmural diffusion coefficients of the free drug with inside the artery wall and V_w is a transmural convective velocity act alongside positive x direction in the tissue.

3.3 Modelling of Drug Binding Procedures

Drug binding interactions are believed to have a significant impact on drug transport as well as retention within the tissue wall in addition to the advection and diffusion. As a result, we use sophisticated two-phase nonlinear saturable binding kinetics, separating drugs that are specifically bound to specific receptor (r) site from those that are non-specifically bound to general *extracellular matrix* (ECM) elements (e) site. Therefore, the resulting advection-diffusion-reaction equations of the non-specific bound drug concentrations $C_{bed}(x, y, t)$, and the specific bound drug concentrations $C_{brd}(x, y, t)$ within the vessel wall, are provided by (McGinty and Pontreli [18]):

$$\frac{\partial C_{bed}}{\partial t} + k^e_{on} K^e_{dc} C_{bed} = k^e_{on} C_{fd} (C^{max}_{bed} - C_{bed}), \tag{3.3}$$

$$\frac{\partial C_{brd}}{\partial t} + k^r_{on} K^r_{dc} C_{brd} = k^r_{on} C_{fd} (C^{max}_{brd} - C_{brd}), \tag{3.4}$$

in which C^{max}_{bed} and C^{max}_{brd} are the local molar concentrations of extracellular matrix and receptor binding sites, k^e_{on} and k^r_{on} are the respective binding on-rate constants, K^e_{dc} and K^e_{dc} are the respective equilibrium dissociation constants.

4. Inclusive Binary 2D-Representation of the Drug Release Pathway

The kinetics of drug release from cardiovascular DES with non-erodible polymer coating is modelled by eqn. (3.1), it is connected to the coupled advection-diffusion model equation as well as nonlinear binding kinetics within the vessel wall represented by the eqns. (3.3)-(3.4). As a result, we reach a complete integrated system of drug release from coronary stent struts and drug transport as well as retention through arterial tissue.

4.1 Illustration of Initial and Boundary Limitations

For approaching the single-layered homogeneous coupled drug transport mechanism described by eqns. (3.1)-(3.4), we wish to set appropriate initial and boundary conditions. The Robin

boundary conditions (McGinty and Pontrelli [19]) are utilised as follows:

$$\frac{\partial C_{fd}}{\partial x} = 0 \text{ on } \Gamma_{t,in} \text{ and } \Gamma_{t,out}, \tag{4.1}$$

where $\Gamma_{t,in}$ and $\Gamma_{t,out}$ are the wall inlet and wall outlet in arterial vessel.

At the adventitia, we assume perfect sink condition for free drug prescribed as:

$$C_{fd} = 0 \text{ on } \Gamma_{uw}. \tag{4.2}$$

The initial conditions are as follows:

$$C_0(x,y,0) = 0,\ C_{fd}(x,y,0) = 0,\ C_{bed}(x,y,0) = 0,\ C_{brd}(x,y,0) = 0. \tag{4.3}$$

In the case of drug-eluting stent, we have considered the continuity of drug mass and mass flux condition prescribed among the stent polymeric coating surface and the arterial tissue interface as:

$$-D_w \frac{\partial C_{fd}}{\partial y} + V_w C_{fd} = -\frac{E_w}{A_{lti} M_w} \frac{\partial C_s}{\partial t} \text{ on } \Omega_{tissue} \cap \Gamma_{st} \tag{4.4}$$

along with

$$-\frac{\partial C_s}{\partial t} = -M_0 K_0 e^{-K_0 t} + \frac{H_s}{2\sqrt{t}}, \tag{4.5}$$

where E_w is the efficiency factor for drug delivery within the arterial tissue wall, A_{lti} is the area of surface of the blood-wall interface and M_w is the molecular weight of drug.

The zero-flux interface condition applied to the lumen blood and adjacent upstream tissue boundary (Vairo *et al*. [27]), so that not a single drug molecule transferred to the blood stream as:

$$\frac{\partial C_{fd}}{\partial y} = 0 \text{ on } \Gamma_{bt}. \tag{4.6}$$

4.2 Information About Non-Dimensionalization Techniques

The collection of space coordinates and time could be transformed into a new set of independent variables during the process of the simplest and most fresh non-dimensional equations as follows:

$$\widetilde{x} = \frac{x}{\delta},\ \widetilde{y} = \frac{y}{r_0},\ \widetilde{t} = \frac{tV_w}{\delta},$$

where r_0, represents the radius of the arterial lumen.

In particular, each and every concentrations of drug have been compared to the original coating dose C_0 as:

$$\widetilde{C}_{fd} = \frac{C_{fd}}{C_0},\ \widetilde{C}_s = \frac{C_s}{C_0}\ \widetilde{C}_\vartheta = \frac{C_\vartheta}{C_0},\ \widetilde{C}_\vartheta^{max} = \frac{C_\vartheta^{max}}{C_0}.$$

Here, $\vartheta = (1,2)$, $\vartheta = 1$ stands for extracellular matrix binding sites (*bed*) and $\vartheta = 2$ stands for receptor binding sites (*brd*).

In the process of adjustments, the subsequent parameters listed as follows:

$$Pe = \frac{r_0 V_w}{D_w},\ Da_e = \frac{\delta C_0 k_{on}^e}{V_w},\ Da_r = \frac{\delta C_0 k_{on}^r}{V_w},\ K_e = \frac{C_0}{K_{dc}^e},\ K_r = \frac{C_0}{K_{dc}^r},$$

$$\lambda = \frac{\delta K_0}{V_w},\ \Lambda = \frac{\lambda M_0}{C_0},\ \Phi = \frac{E_w}{\delta A_{lti} M_w},\ \Psi = \left(\frac{\delta}{V_w}\right)^{\frac{1}{2}} \frac{H_s}{C_0},\ \epsilon = \frac{\delta}{r_0}.$$

With an analogous style and applying the above transformations in dimensional eqns. (3.2)-(3.4), the resulting transformed dimensionless equations as:

$$\frac{\partial C_{fd}}{\partial t}+\epsilon\frac{\partial C_{fd}}{\partial y}+\frac{\partial C_{bed}}{\partial t}+\frac{\partial C_{brd}}{\partial t}=\frac{\epsilon}{Pe}\left[\frac{1}{\epsilon^2}\frac{\partial^2 C_{fd}}{\partial x^2}+\frac{1}{y}\frac{\partial C_{fd}}{\partial y}+\frac{\partial^2 C_{fd}}{\partial y^2}\right], \tag{4.7}$$

$$\frac{\partial C_{bed}}{\partial t}+\frac{Da_e}{K_e}C_{bed}=Da_eC_{fd}(C_{bed}^{max}-C_{bed}), \tag{4.8}$$

$$\frac{\partial C_{brd}}{\partial t}+\frac{Da_r}{K_r}C_{brd}=Da_rC_{fd}(C_{brd}^{max}-C_{brd}). \tag{4.9}$$

In the similar manner, all the dimensional equations of boundary and interface conditions eqns. (4.1)-(4.6) are transformed into the following dimensionless form as:

$$\frac{\partial C_{fd}}{\partial x}=0 \text{ on } \Gamma_{t,in} \text{ and } \Gamma_{t,out}, \tag{4.10}$$

$$C_{fd}=0 \text{ on } \Gamma_{uw}, \tag{4.11}$$

$$-\frac{1}{Pe}\frac{\partial C_{fd}}{\partial y}+C_{fd}=-\Phi\frac{\partial C_s}{\partial t} \text{ on } \Omega_{tissue}\cap\Gamma_{st} \tag{4.12}$$

with

$$-\frac{\partial C_s}{\partial t}=-\Lambda e^{-\lambda t}+\frac{\Psi}{2\sqrt{t}}, \tag{4.13}$$

$$\frac{\partial C_{fd}}{\partial y}=0 \text{ on } \Gamma_{bt}. \tag{4.14}$$

5. Analysis of Solving Procedures

5.1 Adjustment of Radial Dimensions

The following portion contains on the radial coordinate conversion method as:

$$\xi=1+\frac{y-\Gamma_{lw}}{\Gamma_{uw}-\Gamma_{lw}},$$

where, $\Gamma_{lw}=\Gamma_{bt}\cup\Gamma_{st}$, such that the stented irregular region changed into rectangular one, i.e., the cardiovascular tissue domain converted into $[0,L]\times[1,2]$.

5.2 Methodology for Temporal and Spacial Discretization

Therefore all of our transformed governing equations along with the set of initial and boundary conditions are discretized by using of forward-time centred-spaced discretization scheme. Here, introduce $x_i=i\delta x$, $\xi_j=j\delta\xi$ and $t_n=n\delta t$ in which n represents to the time scale, δt, the time progression, δx be the length of a space step across the longitudinal direction and $\delta\xi$ be the length of a space step across the radial direction.

Last but not least, the most recent equations are all numerically solved in a particular fashion. Throughout the present modelling, no well-known package has been implemented, however, FORTRAN language has been efficiently used to design the mathematical algorithm. In order to achieve the steady state level, at least $1,00,000$ iteration stage must be made for MAC framework (Figure 3). When the convergence level for each type of drug mass was 10^{-8}, the steady state had been attained. For information of the numerical procedure in details, involved researchers are suggested to follow Saha and Mandal [24].

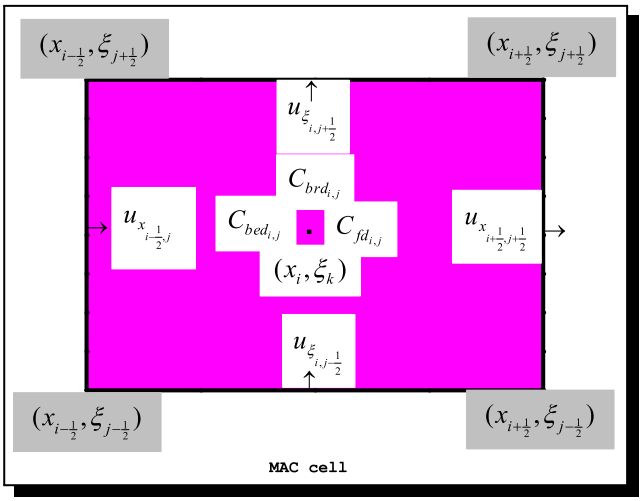

Figure 3. Graphic image of MAC cell for artery wall

Table 1. Recommended measurements for the most significant indicators

Name	Parameter	Value	Source
Strut dimension (cm)	δ	0.01	[2]
Strut coating thickness (cm)	h	5.0×10^{-3}	[21]
Mean lumen radius (cm)	$r_0 (= 15\delta)$	0.15	[2]
Mean wall thickness (cm)	$A_w (= 10\delta)$	0.10	[2]
Interstrut distance (cm)	$\triangle (= 3\delta)$	0.03	[27]
Transmural convective velocity (cm s^{-1})	V_w	5.8×10^{-6}	[14]
Local molar concentrations of ECM site (μM)	C_{bed}^{max}	363	[26]
Local molar concentrations of receptor binding site (μM)	C_{brd}^{max}	3.3	[25]
Binding on-rate constants in ECM site ($\mu M^{-1} s^{-1}$)	k_{on}^{e}	2.6	[26]
Binding on-rate constants in receptor binding site ($\mu M^{-1} s^{-1}$)	k_{on}^{r}	0.2	[5]
Dissociation constant in ECM site (μM)	K_{dc}^{e}	0.002	[26]
Dissociation constant in receptor binding site (μM)	K_{dc}^{r}	0.8	[28]
Transmural free drug diffusivity in tissue wall (cm^2 s^{-1})	D_w	2.5×10^{-6}	[25]
Initial drug concentration in the coating (μg)	C_0	0.98	[25]
Initial pool of first order eluting drug (μg)	M_0	19.73	[25]
Rate constant (d^{-1})	K_0	0.20	[25]
Higuchi rate constant ($\mu g\ d^{-0.5}$)	H_s	4.63	[25]
Efficiency factor of drug transfer	E_w	0.1	[25]
Area of surface of the blood-wall interface (cm^2)	A_{lti}	1.98	[23]
Molecular weight of drug (g mol^{-1})	M_w	914.2	[25]
Dimensionless Peclet number in the tissue wall	Pe	2.0×10^8	Our study
Dimensionless Damköhler number in ECM site	Da_e	5.0×10^3	Our study
Dimensionless Damköhler number in receptor binding site	Da_r	1.0×10^5	Our study
Dimensionless scaling parameter	$\varepsilon = \frac{r_0}{\delta}$	15	Our study

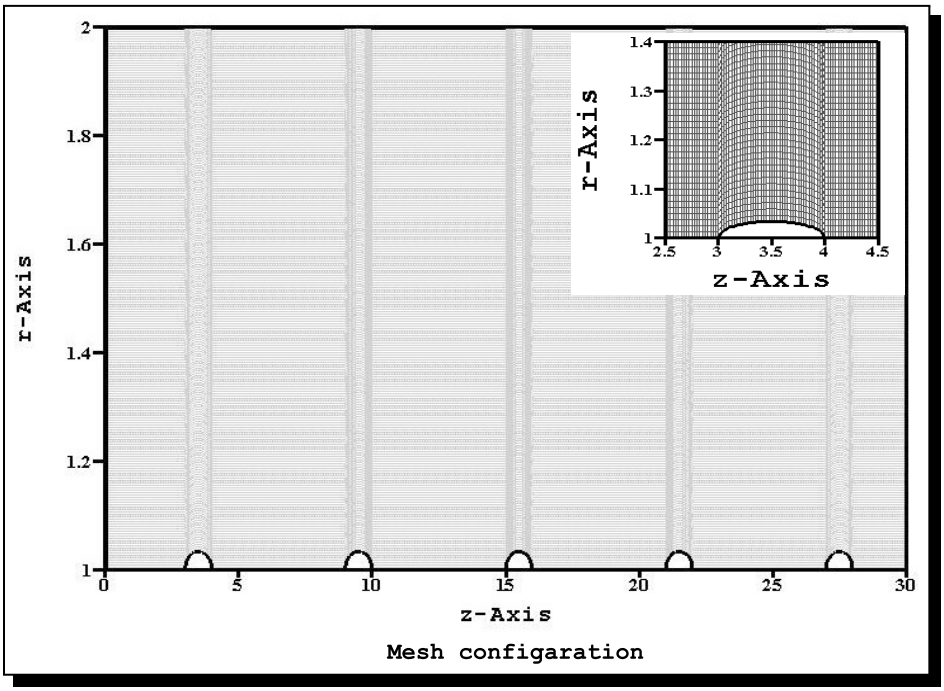

Figure 4. A diagrammatic representation of mesh configuration

6. An Explanation of the Numerical Findings

For getting at the achievable outcomes, we employ identical grids in single-layered homogeneous arterial tissue section having mesh grid sizes 1201×81 (Figure 4). To show the suggested plan has significance, we have implemented time increment $(\Delta t) = 10^{-5}$, and tolerance $= 10^{-8}$, requirements for the MAC arrangement being terminated, considering documented information gathered from the most recent study and readily available scientific journal works [4, 25].

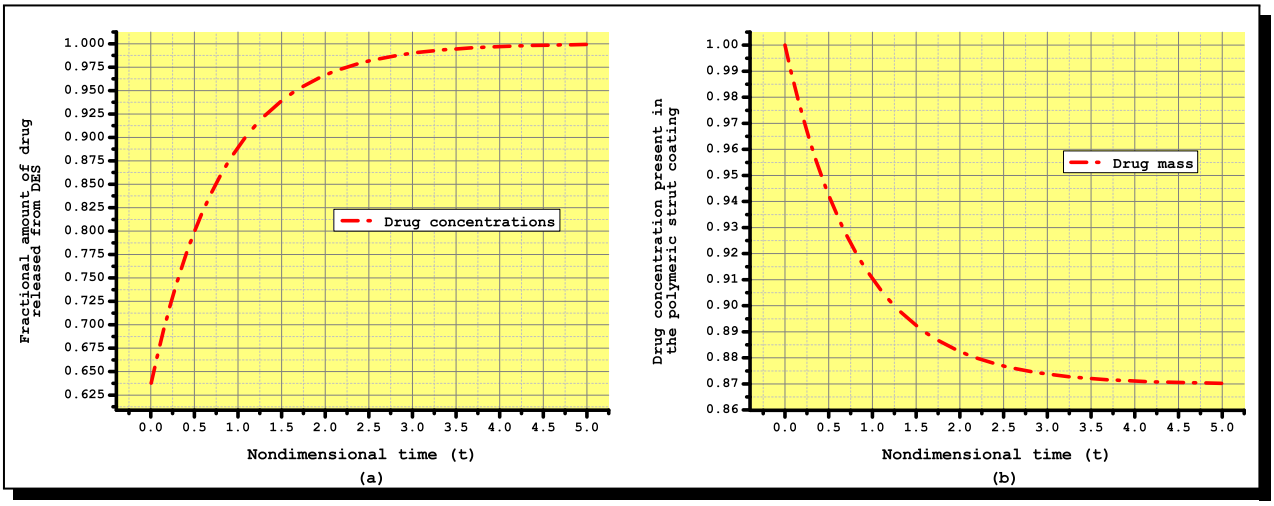

Figure 5. Image of non-dimensional drug mass deliverance from cardiovascular DES with time. (a) Fractional amount of drug release from DES, (b) drug concentration present in the polymetric strut coating

In Figure 5(a) displayed the fractional amount of drug release from DES and Figure 5(b) displayed the drug concentration present in the polymer strut coating for a period of dimensionless time = 5. Figure 5(a) indicates that the amount of drug release from the stent strut is increases with increasing time and reaches the saturated value after the dimensionless time = 5. First of all, these results implies that, in general, the procedure of proceeds very fast in this type of stent arrangement. Figure 5(b) suggests that the presence concentrations of drug within the polymer coating is slow decreases with increasing time. Interestingly, after dimensionless time $t = 5$ more than 80% of the primary drug amount is still remains in the polymer stent coating. A strong connection amongst the present investigation and the existing prior research appears through the evaluations [19].

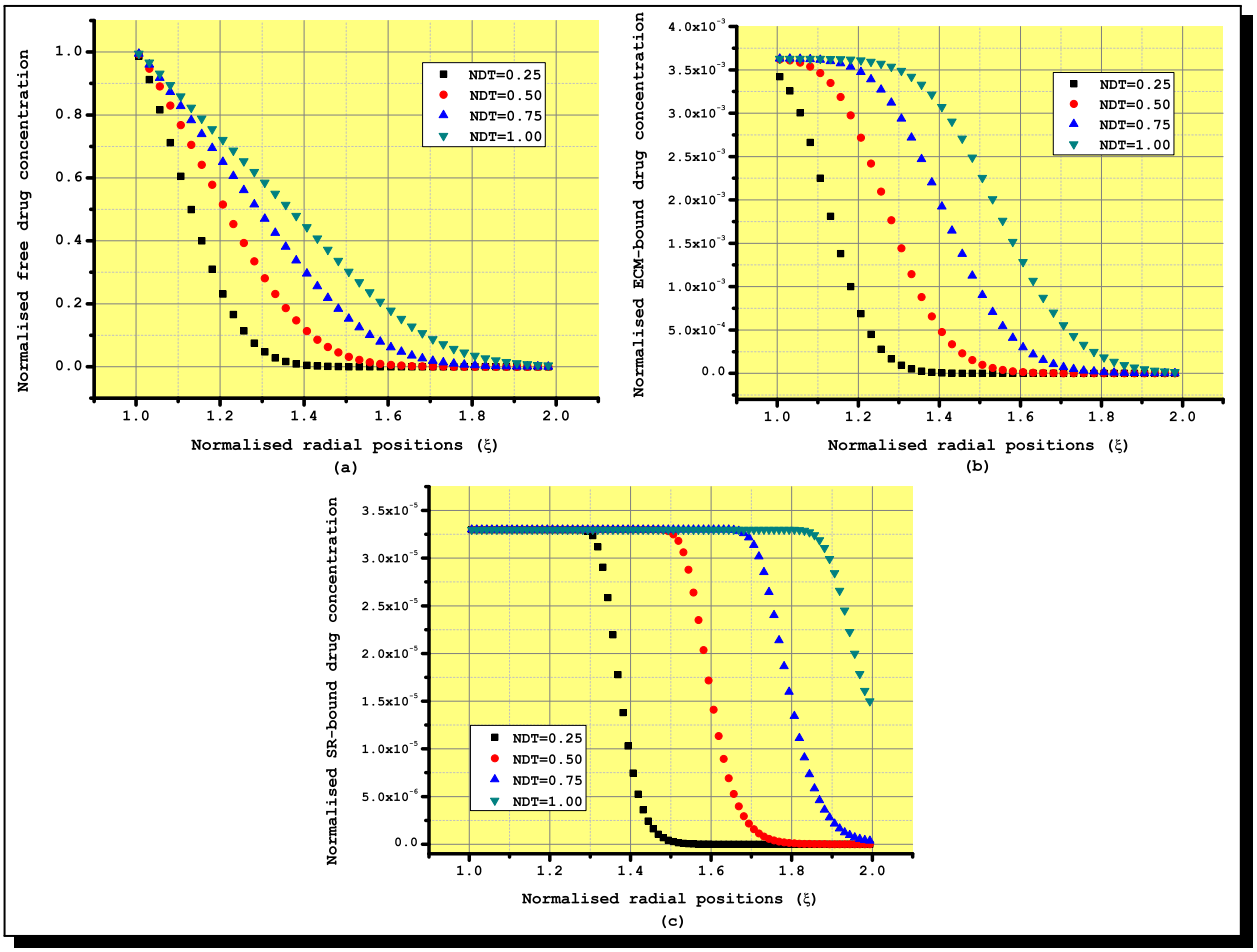

Figure 6. Diagram of radial position variant normalized drug masses for different times. (a) free drug, (b) non-specific bound drug and (c) specific bound drug concentration

We exhibit modelled concentration patterns of free drug, non-specific bound drug and specific bound drug concentrations in Figure 6(a-c) to assess the influence of interpreting specific and non-specific binding as two distinct phases. It is observed from Figure 6(a) that, the free drug concentrations, C_{fd}, immediately bind to non-specific and specific locations after entering into arterial tissue region ($r = 1$) within the free phase. In Figures 6(b,c), it is also cleared that both the drugs (free and ECM-bound) passes through the arterial tissue, becomes bound to specific

binding sites, and under goes absorbtion at the adventitial layer border line ($x = 2$), causing the free, C_{fd}, and non-specific bound drug, C_{bed}, mass patterns to increase to highest point until gradually declining over the course of time. The bound drug masses throughout the ECM binding sites are nearly second order of magnitude higher than those inside the specific receptor binding sites, that are consequently hundred times smaller than the free drug mass, despite the fact that the free (C_{fd}) and non-specific bound drug (C_{bed}) mass pattern geometries are identical in nature. This findings is not inconsistent with Tzafriri *et al*. [26].

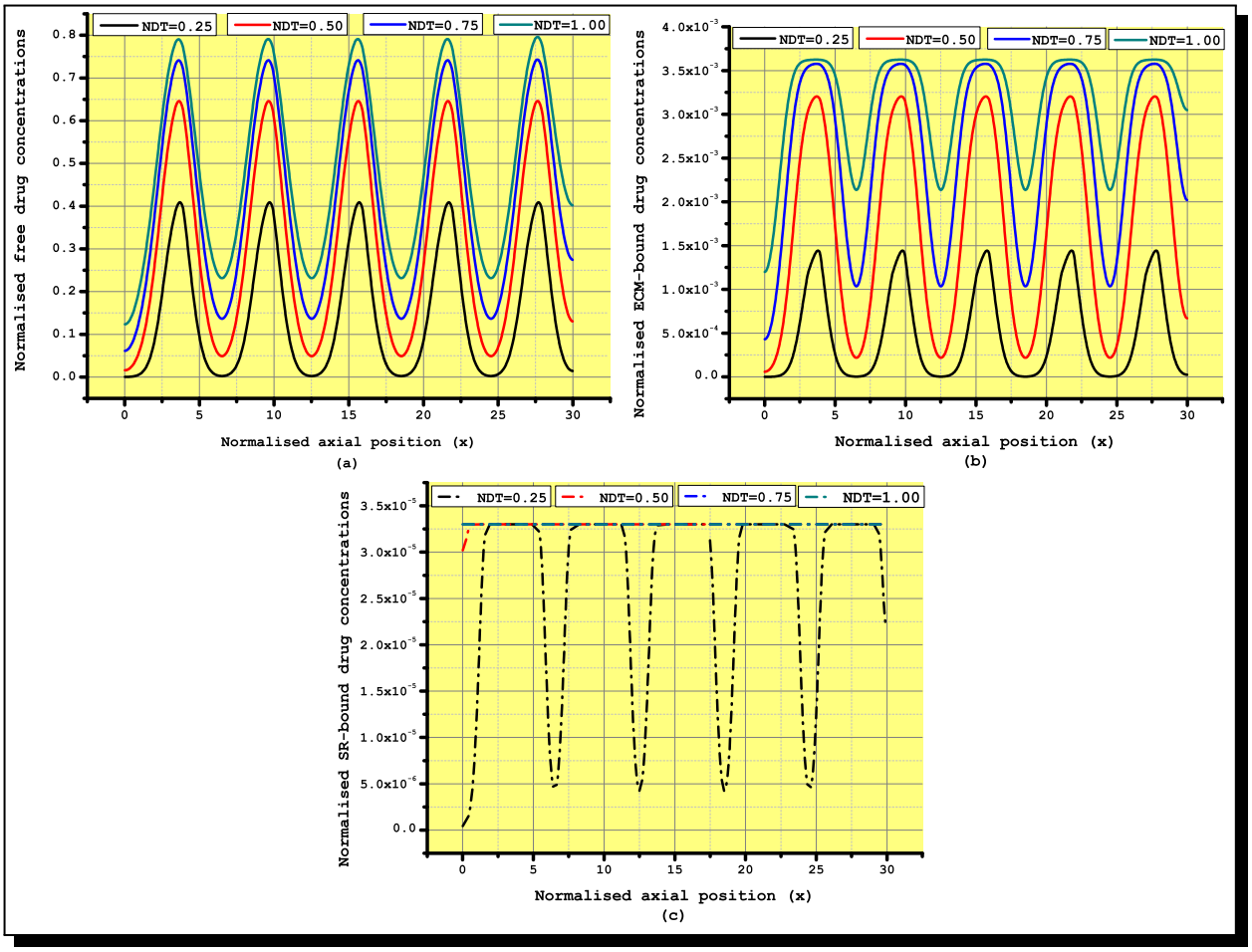

Figure 7. Diagram of axial position variant normalized drug masses for different times. (a) free drug, (b) non-specific bound drug, (c) specific bound drug

The axial concentration profiles of normalised free, non-specific bound drug and specific bound drug mass were depicted in Figures 7(a-c) respectively, varied with different times. Figures 7(a-c) shows that all the symmetry concentration patterns within the arterial tissue increase with increasing time. Models showed that two separate recirculating areas develop near and far from multiple stent struts, with the latter being substantially bigger than the former. Thus, the results indicate that the aforementioned regions produce compartments of drug-filled blood that are stagnant, allowing drugs to build up at luminal-artery contact and then enter the arterial tissue wall, which has the identical viewpoint as Tzafriri *et al*. [25].

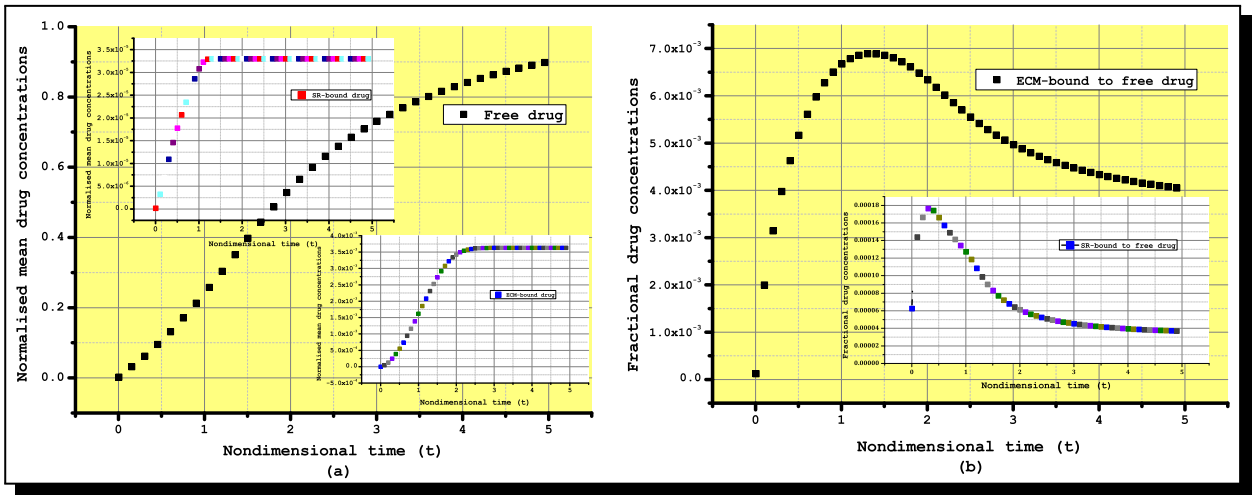

Figure 8. (a) Variation of normalized mean free drug, non-specific bound drug and specific bound mass in arterial tissue wall with time (a magnified version of the non-specific and specific bound drug mass during the non-dimensional time 5 is shown in the inset), (b) Variation of fractional tissue bound drug concentration: non-specific bound to free drug and specific bound to free drug (a magnified version of fractional specific bound drug mass to free drug mass during the non-dimensional time 5 is shown in the inset)

Temporal variations of normalised mean free, non-specific (inset) and specific (inset) drug concentrations are presented in Figure 8(a). It is appears that the level of normalised mean drug mass that is non-specific and specific bound drug mass increase from zero to a maximum value and then gradually saturated over time, but when time is taken into account, the amount of normalised mean free drug mass steadily rises. It is important to note that non-specific bound drug mass peaks later than specific bound drug mass does, and non-specific bound phase contains the most drug mass compared to the specific bound phase. These findings are in good accordance with those reported by Tzafriri *et al*. [25]. Temporal variations of normalised fractional tissue non-specific bound to free drug and specific bound to free drug (inset) are depicted in Figure 8(b). It is reveals that the level of normalised fractional tissue bound drug concentrations (both non-specific bound to free drug and specific bound to free drug) increase from zero to a maximum value and then slowly decreases over time. It is also notable that fraction of non-specific bound drug mass to free drug mass peaks later than specific bound drug mass to free drug mass does. Here, too, we also see that the normalise average free drug mass in case of the single phase drug binding model is always higher than that of the double-phased drug binding system, this fact is just due to less conversion of free drug concentration into bound drug concentration form in the single-phased binding model. That happens to be consistent with McGinty and Pontrelli [18].

Figures 9(a-c) help to depicted the geographical distribution pattern within a rectangular region. The above mentioned diagrams unambiguously show that drug mass steadily release from strut surfaces and progressively distributed across the arterial tissue region. Additionally, the rate of binding accelerates with passing time as long as the binding locations becomes overwhelmed. This findings also demonstrate that drug delivery from the stent strut to the arterial tissue wall is too small to cover a significant portion of non-specific binding sites

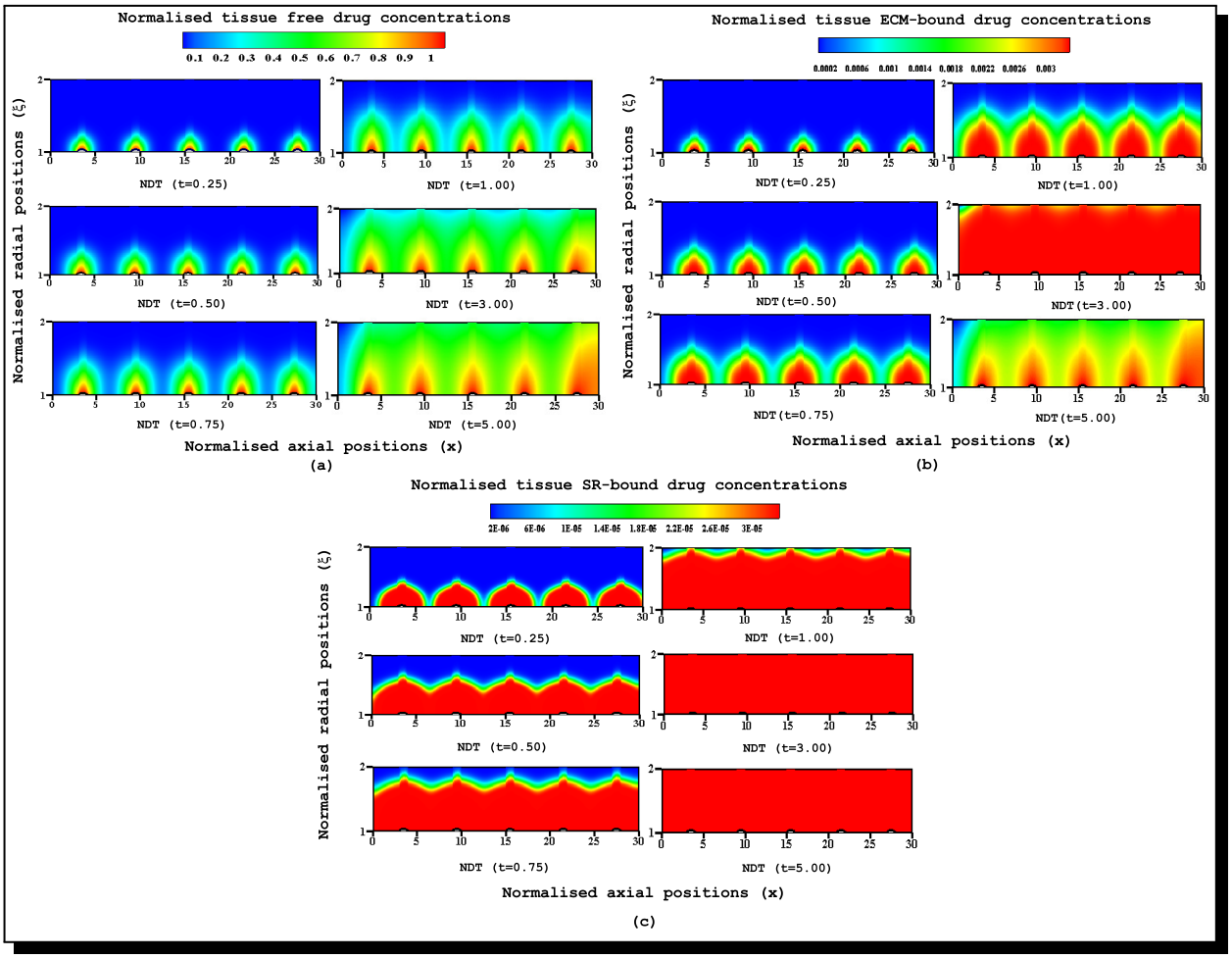

Figure 9. Spectacular image profile of drug mass in arterial vessel wall for different time scales. (a) free drug, (b) non-specific bound drug, (c) specific bound drug

but sufficiently high to saturated specific binding sites. As a result, the conclusions reached by Balakrishnan *et al*. [3] are supported.

7. Summary and Opportunities for Future Exploration

The model studies initially contrast the intravascular drug distribution eluted from a biodegradable polymer coated stent strut. The influence of interstitial fluid flow and strut embedment on drug transport and distribution are then independently examined using the drug-coated stent model. Unless otherwise specified, half-embedded drug eluting stent with time dependent drug release kinetics of Higuchi model is taken into account in the model simulations. The pattern of drug release in the coating, mean drug concentrations in the wall of arteries for the varies drug types, and spatial drug concentrations distribution in the vascular wall are all provided based on the computational findings. The impact of various important factors is investigated in this article through analysis of three-phase (free, non-specific and specific binding sites) single-layered drug elution model with a half-embedded drug eluting stent. The

finding show that more precise outcomes in drug transport and retention within the arterial wall have been achieved. This enhanced simulation may be useful for future study for bettering the functioning of DES^s in respect to safety and efficacy because most computational and numerical investigations disregard either half-embedement of strut or three-phased drug configurations.

The following are the main findings' highlights:

- The effects on drug delivery as well as retention features of the incorporation of single-layered homogeneous artery wall and cardiovascular half-embedded drug-eluted stent struts are magnificent.
- Right up to a certain level, the standardized drug amounts of both specific and non-specific structures decreases, but after this level, an inverted pattern is seen as a result of cellular refusal of pharmaceutical compounds.
- On analyzing time-dependent dynamics of the release of drugs in the vessel wall zone, the standardized drug concentrations of non-specific binding elements are significantly more than the specific binding zones.
- As long as an equilibrium level of sites of binding, the progress of binding accelerates with the passing of time.

The main goal of this work is to provide an appropriate drug delivery mechanism inside the artery wall with time-varying release dynamics from half-embedded drug-eluting struts. While conducting the present study, a variety of simplified versions were adopted as way to avoid the complexity on in-vivo vascular pharmacokinetics. Here, blood flow of arterial lumen has not been taken into account, despite the fact that it affects the transportation and retention of free drug mass. It is anticipated that more realistic 3D model geometry will provide a better understanding based on the results obtained utilising the simple geometry.

Acknowledgements

This research work received assistance on behalf of Department of Mathematics and Department of Physics, Suri Vidyasagar College (affiliated to the University of Burdwan), Suri, Birbhum, West Bengal, India. The authors also express their gratitude to Prof. Prashanta Kumar Mandal, Department of Mathematics, Visva-Bharati University, Shantiniketan, Birbhum, West Bengal, India for his fruitful suggestions and advices. The authors especially convey their thankful acknowledgment to the knowledgeable reviewers for their thorough examination and recommendations.

Competing Interests

The authors declare that they have no competing interests.

Authors' Contributions

All the authors contributed significantly in writing this article. The authors read and approved the final manuscript.

References

[1] G. Acharya and K. Park, Mechanisms of controlled drug release from drug-eluting stents, *Advanced Drug Delivery Reviews* **58**(3) (2006), 387 – 401, DOI: 10.1016/j.addr.2006.01.016.

[2] B. Balakrishnan, J. Dooley, G. Kopia and E. R. Edelman, Thrombus causes fluctuations in arterial drug delivery from intravascular stents, *Journal of Controlled Release* **131**(3) (2008), 173 – 180, DOI: 10.1016/j.jconrel.2008.07.027.

[3] B. Balakrishnan, J. F. Dooley, G. Kopia and E. R. Edelman, Intravascular drug release kinetics dictate arterial drug deposition, retention, and distribution, *Journal of Controlled Release* **123**(2) (2007), 100 – 108, DOI: 10.1016/j.jconrel.2007.06.025.

[4] B. Balakrishnan, A. R. Tzafriri, P. Seifert, A. Groothuis, C. Rogers and E. R. Edelman, Strut position, blood flow, and drug deposition: Implications for single and overlapping drug-eluting stents, *Circulation* **111**(22) (2005), 2958 – 2965, DOI: 10.1161/CIRCULATIONAHA.104.512475.

[5] B. E. Bierer, P. S. Mattila, R. F. Standaert, L. A. Herzenberg, S. Burakoff, G. Crabtree and S. L. Schreiber, Two distinct signal transmission pathways in T lymphocytes are inhibited by complexes formed between an immunophilin and either FK506 or rapamycin, *Proceedings of the National Academy of Sciences* **87**(23) (1990), 9231 – 9235, DOI: 10.1073/pnas.87.23.9231.

[6] A. Borghi, E. Foa, R. Balossino, F. Migliavacca and G. Dubini, Modelling drug elution from stents: Effects of reversible binding in the vascular wall and degradable polymeric matrix, *Computer Methods in Biomechanics and Biomedical Engineering* **11**(4) (2008), 367 – 377, DOI: 10.1080/10255840801887555.

[7] F. Bozsak, D. Gonzalez-Rodriguez, Z. Sternberger, P. Belitz, T. Bewley, J. M. Chomaz and A. I. Barakat, Optimization of drug delivery by drug-eluting stents, *PloS One* **10**(6) (2015), e0130182, DOI: 10.1371/journal.pone.0130182.

[8] M. A. Costa and D. I. Simon, Molecular basis of restenosis and drug-eluting stents, *Circulation* **111**(17) (2005), 2257 – 2273, DOI: 10.1161/01.CIR.0000163587.36485.A7.

[9] J. Escuer, I. Aznar, C. McCormick, E. Peña, S. McGinty and M. A. Martínez, Influence of vessel curvature and plaque composition on drug transport in the arterial wall following drug-eluting stent implantation, *Biomechanics and Modeling in Mechanobiology* **20** (2021), 767 – 786, DOI: 10.1007/s10237-020-01415-3.

[10] GBD 2017 Causes of Death Collaborators, Global, regional, and national age-sex-specific mortality for 282 causes of death in 195 countries and territories, 1980–2017: A systematic analysis for the Global Burden of Disease Study 2017, *The Lancet* **392**(10159) (2018), 1736 – 1788, DOI: 10.1016/S0140-6736(18)32203-7.

[11] M. Grassi, G. Pontrelli, L. Teresi, G. Grassi, L. Comel, A. Ferluga and L. Galasso, Novel design of drug delivery in stented arteries: A numerical comparative study, *Mathematical Biosciences and Engineering* **6**(3) (2009), 493 – 508, DOI: 10.3934/mbe.2009.6.493.

[12] T. Higuchi, Mechanism of sustained-action medication. Theoretical analysis of rate of release of solid drugs dispersed in solid matrices, *Journal of Pharmaceutical Sciences* **52**(12) (1963), 1145 – 1149, DOI: 10.1002/jps.2600521210.

[13] S. Hossainy and S. Prabhu, A mathematical model for predicting drug release from a biodurable drug-eluting stent coating, *Journal of Biomedical Materials Research Part A* **87A**(2) (2008), 487 – 493, DOI: 10.1002/jbm.a.31787.

[14] Z. J. Huang and J. M. Tarbell, Numerical simulation of mass transfer in porous media of blood vessel walls, *American Journal of Physiology-Heart and Circulatory Physiology* **273**(1) (1997), H464 – H477, DOI: 10.1152/ajpheart.1997.273.1.H464.

[15] C.-W. Hwang, D. Wu and E. R. Edelman, Physiological transport forces govern drug distribution for stent-based delivery, *Circulation* **104**(5) (2001), 600 – 605, DOI: 10.1161/hc3101.092214.

[16] S. McGinty, A decade of modelling drug release from arterial stents, *Mathematical Biosciences* **257** (2014), 80 – 90, DOI: 10.1016/j.mbs.2014.06.016.

[17] S. McGinty, S. McKee, C. McCormick and M. Wheel, Release mechanism and parameter estimation in drug-eluting stent systems: Analytical solutions of drug release and tissue transport, *Mathematical Medicine and Biology: A Journal of the IMA* **32**(2) (2015), 163 – 186, DOI: 10.1093/imammb/dqt025.

[18] S. McGinty and G. Pontrelli, A general model of coupled drug release and tissue absorption for drug delivery devices, *Journal of Controlled Release* **217** (2015), 327 – 336, DOI: 10.1016/j.jconrel.2015.09.025.

[19] S. McGinty and G. Pontrelli, On the role of specific drug binding in modelling arterial eluting stents, *Journal of Mathematical Chemistry* **54** (2016), 967 – 976, DOI: 10.1007/s10910-016-0618-7.

[20] C. M. McKittrick, S. Kennedy, K. G. Oldroyd, S. McGinty and C. McCormick, Modelling the impact of atherosclerosis on drug release and distribution from coronary stents, *Annals of Biomedical Engineering* **44**(2) (2016), 477 – 487, DOI: 10.1007/s10439-015-1456-7.

[21] F. Migliavacca, F. Gervaso, M. Prosi, P. Zunino, S. Minisini, L. Formaggia and G. Dubini, Expansion and drug elution model of a coronary stent, *Computer Methods in Biomechanics and Biomedical Engineering* **10**(1) (2007), 63 – 73, DOI: 10.1080/10255840601071087.

[22] R. Mongrain, I. Faik, R. L. Leask, J. Rodés-Cabau, É. Larose and O. F. Bertrand, Effects of diffusion coefficients and struts apposition using numerical simulations for drug eluting coronary stents, *Journal of Biomechanical Engineering* **129**(5) (2007), 733 – 742, DOI: 10.1115/1.2768381.

[23] K. L. Napoli and P. J. Taylor, From beach to bedside: History of the development of sirolimus, *Therapeutic Drug Monitoring* **23**(5) (2001), 559 – 586, DOI: 10.1097/00007691-200110000-00012.

[24] R. Saha and P. K. Mandal, Modelling time-dependent release kinetics in stent-based delivery, *Journal of Exploratory Research in Pharmacology* **3**(2) (2018), 61 – 70, DOI: 10.14218/JERP.2018.00001.

[25] A. R. Tzafriri, A. Groothuis, G. S. Price and E. R. Edelman, Stent elution rate determines drug deposition and receptor-mediated effects, *Journal of Controlled Release* **161**(3) (2012), 918 – 926, DOI: 10.1016/j.jconrel.2012.05.039.

[26] A. R. Tzafriri, A. D. Levin and E. R. Edelman, Diffusion-limited binding explains binary dose response for local arterial and tumour drug delivery, *Cell Proliferation* **42**(3) (2009), 348 – 363, DOI: 10.1111/j.1365-2184.2009.00602.x.

[27] G. Vairo, M. Cioffi, R. Cottone, G. Dubini and F. Migliavacca, Drug release from coronary eluting stents: A multidomain approach, *Journal of Biomechanics* **43**(8) (2010), 1580 – 1589, DOI: 10.1016/j.jbiomech.2010.01.033.

[28] M. A. Wear and M. D. Walkinshaw, Determination of the rate constants for the FK506 binding protein/rapamycin interaction using surface plasmon resonance: An alternative sensor surface for Ni^{2+}-nitrilotriacetic acid immobilization of His-tagged proteins, *Analytical Biochemistry* **371**(2) (2007), 250 – 252, DOI: 10.1016/j.ab.2007.06.034.

[29] X. Zhu, *Mathematical Modeling and Simulation of Intravascular Drug Delivery from Drug-Eluting Stents with Biodegradable PLGA Coating*, Ph.D. Thesis, Massachusetts Institute of Technology, USA.